Rev. Int. Contam. Ambie. 40, 313-229, 2024
https://doi.org/10.20937/RICA.55051

POTENTIAL OF CHITOSAN AND ACTIVATED CARBON BIOCOMPOSITES FOR REMOVING ENROFLOXACIN AND OXYTETRACYCLINE FROM WATER

Potencial de biocompositos de quitosano y carbón activado para remover enrofloxacina y oxitetraciclina de agua

José Manuel MOLINA-AMAYA[1], José Antonio ÁVILA-REYES[1]*, Eli Amanda DELGADO-ALVARADO[1], Laura Silvia GONZÁLEZ-VALDEZ[1], Rene TORRES-RICARIO[1], Marlon ROJAS-LÓPEZ[2], Norma ALMARAZ-ABARCA[1] and Marcela Verónica GUTIÉRREZ-VELÁZQUEZ[1]

[1] Instituto Politécnico Nacional, Centro Interdisciplinario de Investigación para el Desarrollo Integral Regional unidad Durango, Sigma 119, 20 de Noviembre II, Durango, C.P. 34220, Durango, Mexico.
[2] Instituto Politécnico Nacional, Centro de Investigación en Biotecnología Aplicada, Ex Hacienda de San Juan Molino, Carretera Estatal Santa Inés, Tecuexcomac-Tepetitla. Kilómetro 1.5, Tepetitla, C.P. 90700, Tlaxcala, Mexico.

*Author for correspondence: jaavre@yahoo.com.mx

(Received: June 2023; accepted: September 2023)

Key words: adsorption, water treatment, recalcitrant pollutants, functional groups.

ABSTRACT

Enrofloxacin (ENRO) and oxytetracycline (OTC) are two antibiotics, which are difficult to remove by conventional water treatment methods. The characteristics of the biocomposites suggest that they could represent an alternative for the removal of this type of substances through adsorption processes. The current study aimed to determine and compare the potential of biocomposites formed with chitosan and different concentrations of activated carbon (AC) with a particle size of 500 nm, prepared from agave bagasse, to remove enrofloxacin and oxytetracycline solved in water. The effectiveness of the addition of different concentrations of AC (0, 0.5, 2 and 5% w/v) to chitosan was evaluated by morphological analysis using scanning electron microscopy (SEM). The detection of the characteristic functional groups carried out by Fourier transform infrared spectroscopy (FTIR) indicated that the nanoparticles of AC were attached in the chitosan biocomposite, and stable chemical crosslinking was formed during the polymerization process. The removal test of ENRO (10 mg/mL) and OTC (10 mg/mL) in a water was performed by a gradient method of high-performance liquid chromatography (HPLC). The results showed that the addition of AC to chitosan formed a biocomposite with maximum capacity to remove 59.3% of OTC (contact time 2 h at 100 rpm, 4 g biocomposite/L solution, pH 6-7, 30 ºC), and a maximum removal of 50.3% of ENRO (contact time 2 h at 100 rpm, 4 g biocomposite/L solution, pH 6, 30 ºC). Biocomposites formed by chitosan and agave activated carbon can support the development of tools for the removal of recalcitrant antibiotics from water bodies.

Palabras clave: adsorción, tratamiento de agua, contaminantes emergentes, grupos funcionales.

RESUMEN

La enrofloxacina (ENRO) y la oxitetraciclina (OTC) son dos antibióticos difíciles de eliminar por métodos convencionales de tratamiento de agua. Las características de los biocompositos sugieren que podrían ser una alternativa para la remoción de este tipo de sustancias por procesos de adsorción. El objetivo del presente estudio fue determinar y comparar el potencial de los biocompositos formados con quitosano y diferentes concentraciones de carbón activado (CA) con un tamaño de partícula de 500 nm, preparados a partir de bagazo de agave, para remover enrofloxacina y oxitetraciclina en solución acuosa. Se evaluó la efectividad de la adición de diferentes concentraciones de CA (0, 0.5, 2 y 5 % p/v) al quitosano mediante análisis morfológico usando microscopía electrónica de barrido. La detección de los grupos funcionales característicos llevada a cabo mediante espectroscopía infrarroja por transformada de Fourier (FTIR), mostró que las nanopartículas de CA están unidas al biocomposito de quitosano sugiriendo un entrecruzamiento químico estable, formado durante el proceso de polimerización. La prueba de eliminación de ENRO (10 mg/mL) y OTC (10 mg/mL) en agua se realizó mediante un método en gradiente de cromatografía líquida de alta resolución (HPLC). Los resultados mostraron que la adición de CA al quitosano formó un biocomposito con capacidad máxima de remover 59.3 % de OTC (tiempo de contacto 2 h a 100 rpm, 4 g biocomposito/L solución, pH 6-7, 30 ºC) y un porcentaje 50.3 % como remoción máxima de ENRO (2 h tiempo de contacto a 100 rpm, 4 g biocomposito/L solución, pH 6, 30 ºC). Los biocompositos formados por quitosano y carbón activado de agave pueden apoyar el desarrollo de herramientas para la eliminación de antibióticos recalcitrantes de los cuerpos de agua.

INTRODUCTION

The increased industrial, agricultural, and urban activities have generated an increase of polluting waste (Guerrero-Pérez et al. 2012). Antibiotics, such as enrofloxacin (ENRO) and oxytetracycline (OTC) used in veterinary industry are not eliminated or degraded during wastewater treatment processes and remain in water bodies (Babić et al. 2006), generating potential risk to human health and environmental damage (Martín et al. 2023).

ENRO and OTC are widely used in agriculture, aquaculture, and livestock to treat many infections. These drugs are used as food additives or in water to maintain the optimal health of food-producing animals. Its use will depend on the animal treated, production volume, and pathogens to be eliminated. Some are excreted in their active form via urine or feces after administration. Due to its recent detection in low concentrations (µg/L, ng/L), knowledge about its occurrence is still generated, fate, behavior, risk assessment, and ecological and human effects (Vargas-Berrones et al. 2020). Both antibiotics have been related to the development of resistance in human and animal pathogens, contributing to increased morbidity (Alanazi et al. 2021). The presence of OTC residues can produce damage to the liver and toxic effects (Yang et al. 2013), as well as allergic reactions, bioaccumulation, and intestinal flora imbalance in the case of ENRO (Wu et al. 2023). For the above reasons, the development of strategies to eliminate or reduce the impacts of these substances become a relevant issue. There are various physicochemical methods and technologies in water treatment that include advance oxidation, photocatalytic degradation, membrane filtration, electrochemical oxidation, and biocomposites adsorption for removal drugs in water (Rahman et al. 2022).

Due to their low cost and local availability, natural materials such as chitosan, zeolites, clay, oxides, and carbon are classified as good options for synthesis adsorbents (Babel et al. 2003). However, like any other technology, biocomposite removal has disadvantages such as a decrease in efficiency due to operating without pressure, pH variations or need high operating temperatures (Esfahani et al. 2019).

Attention has been paid to the development of biocomposites formed by a combination of materials, in which one of them acting as a matrix, merging the best intrinsic characteristics of both materials (mechanical, thermal, electrical, and magnetic properties) to improve pollutants removal from water (Nisticò et al. 2020).

The precursors used for the synthesis of activated carbon (AC) must have a high carbon content. Agricultural and industrial wastes are suitable materials

for producing AC because they contain high carbon contents and are generated in large quantities at low cost. Several studies have reported that it is possible to produce high-quality AC from lignocellulosic waste (Lewoyehu 2021). There are many residual lignocellulosic materials from the agroindustry that could be used as precursors to produce AC (González-García. 2018). Mixtures of agriculture wastes have also been used as feedstock to synthetize AC used in pesticide removal (Hussain et al. 2023). Some of them are *Eucalyptus* biomass (Shi et al. 2023), fruit shell (Anita et al. 2023), peanut hulls, and corn hulls (Neme et al. 2022). One biomass option for AC synthesis is bamboo biomass, which is rich in lignocellulose content, making it a good raw material (Suhaimi et al. 2022). Research has been done on methylene blue removal using AC synthetized from *Acacia erioloba* (Daniel et al. 2023).

Other studies have shown that tarap residues (*Artocarpus odoratissimus*) have been successfully used as adsorbents for the removal of heavy metals and dyes (Mohamad Zaidi et al. 2021). Studies have also been made on the synthesis of AC from sheep manure for the adsorption of drugs in water (Dilekoglu et al. 2023).

Agave bagasse is one of the main wastes generated by the tequila and mezcal industries. Total production was 788.2 thousand tons in 2014 to 941.8 tons in 2016. Due to its low cost, availability, and avoidance of contamination problems, it can be used for the synthesis of AC (Robles et al. 2018).

AC is a microcrystalline and non-graphitic material, prepared by carbonizing of organic materials, especially of lignocellulosic origin, which are subjected to a physical (thermal treatment) or chemical ($ZnCl_2$, H_3PO_4, KOH, or NaOH) activation process. Activation process increase its porosity, internal surface, active sites, and diversify its superficial chemical functional groups, resulting in a material with a higher capacity to adsorb different molecules (Dizbay-Onat et al. 2017), such as heavy metals, phenolics, drugs, and organic matter (Teow 2019).

The transformation of a material on a nanometric scale of carbon crystals increases its thermal, mechanical, and chemical properties, improving its potential for application in medicine, electronics, chemistry, and engineering. This is why the synthesis analysis and testing of these materials are necessary (Kulkarni 2015).

At present, biopolymers are valued for their adsorptive capacity and as a support material. Chitosan is a biodegradable polysaccharide with a high adsorption capacity due to its amine and hydroxyl surface functional groups. However, its low mechanical stability is a significant disadvantage. One solution to these drawbacks is the preparation of chitosan biocomposites, combining it with an adsorbent with mechanical and chemical resistance (Sharififard et al. 2018).

The union of both materials increases the contact surface and modifies the surface charges, which increases the adsorption capacity and promotes linkage mechanisms (Tee et al. 2023).

The current study aimed to physicochemically characterize the AC, chitosan, and biocomposite formed by both materials to evaluate the removal potential of ENRO and OXY solved in water.

MATERIALS AND METHODS

Preparation of AC

Samples of agave bagasse resulting from the mezcal manufacturing industry were donated by producers of Durango, Mexico (23º51′N 104º15′W). Samples were collected during the mezcal production cycle in August 2019. The agave bagasse was washed with distilled water to avoid impurities and dried at 60 ºC to a constant weight. Different temperatures were used for the physical activation of the agave bagasse (400-800 ºC), according to Pallarés et al. (2018). Whereas, for the chemical activation, the range of impregnation ratio (IR) of H_3PO_4 was evaluated considering the acid reduction criteria reported by Üner and Bayrak (2018). The AC preparation was carried out using previously reported procedures with some modifications. Then, the samples were activated with H_3PO_4 in a muffle furnace with an IR between 0.3-1.25 (w/w), carbonation times 30-120 min. Finally, the AC were cooled to room temperature, washed with 1 M NaOH until pH reached 6-7. The AC was dried in an oven at 80 ºC for 12 h and stored in plastic containers (Neme et al. 2022).

Nanometric grinding

AC was conditioned by hand grinding (50 g for one hour). After this, a sample was taken, and the average particle size was determined. A sample of AC was analyzed with dynamic light scattering (DLS) equipment (Horiba LA-910, Japan). The result of the particle sizes was statistically expressed as a mean value derived from the intensity distribution of the scattered light called the Z average. The average particle size achieved was 31.1256 µm. To reach a nanometric scale particle size of 500 nm, 2 g of the grounded material was combined with 1.5 L of

distilled water; the dispersion was subjected to an ultrasound bath for 30 minutes to avoid agglomeration and submitted to a high-energy grinding process for four h in a Neos System LabStar equipment (Netzsch – Feinmahltechnik GmbH, Germany) at 3600 RPM. This procedure was repeated thrice to obtain a final sample of 5 g of AC.

Preparation of biocomposites

For the preparation of the biocomposites, mixtures of 25 mL of low molecular weight chitosan (Sigma-Aldrich, St. Louis, MO, USA) and 0, 0.5, 2, and 5% (w/v) of the selected AC were prepared. Chitosan and AC were mixed in acetic acid (4% v/v) (Betancourt-Galindo et al. 2014). Samples were prepared in a Branson brand fixed frequency ultrasonic bath (Branson M1800 Bransonic, CT, USA) to ensure the homogeneity of the mixture (López-Muñoz 2022). The solution was prepared to form a viscous gel and stirred for two h at 40 kHz at a temperature of 60 ºC and precipitated in 1 M NaOH. The beads were filtered from the NaOH bath and washed with tri-distilled water to neutral pH, dried at room temperature and measured until obtained an average diameter of 1 mm (Sharififard et al. 2012).

Biocomposite pH measurement was made using the potentiometric method. 5 g of sample was mixed in water, and the pH was measured using a pH meter Hannah-18424. Electrical conductivity was measured using the electrometric method with the help of a Con5 LaMotte conductivity meter (Tee et al. 2023).

Elemental characterization

The organic matter content (C_2) of AC, chitosan, and biocomposites was determined by the AS-7 method Walkley and Black based on the Official Mexican Standard NOM-021-RECNAT-2000 (SEMARNAT 2002). The micro Kjeldhal method AOAC Official Method 960.52-1961 (AOAC 2010) was used to determine the total nitrogen (N_2) content.

Scanning electron microscopy (SEM)

To obtain the images of the surface morphology of AC and biocomposites, samples were analyzed by SEM (FEI Nova NanoSEM 200, USA). Two-electron SEM signals and a backscattered electron detector were used. The instrument was operated on the parameters on mode Surface Specific (SS) 5.0 kV, pressure 0.60 mbar with magnifications of 500, 1000, 2000 and 2500 times for the AC samples, and 2000 for biocomposites, according to Benedetti et al. (2017).

Fourier transform infrared spectroscopy (FTIR)

FTIR was used to identify the chemical groups present on the surface of samples, which was revealed by identifiable bands within the infrared absorption (Fathizadeh et al. 2019). Samples of the solid and dry materials (AC and chitosan biocomposites) were placed on the diamond crystal of attenuated total reflectance (ATR) accessory of the FTIR/NIR equipment (Perkin Elmer FTIR/NIR Frontier, Mexico). The spectra were collected between the interval of wavenumbers of 4000-400 cm^{-1}, with 256 scans, at a resolution of 4 cm^{-1} (Baig et al. 2019).

Preparation of antibiotic solutions and removal treatments

To evaluate the removal capacity of prepared biocomposites, antibiotic solutions in high concentration were prepared by dissolving the corresponding solid standards in 1 L of tri-distilled water and homogenized manually for 2 min (Esfahani et al. 2019), in the case of ENRO the pH was adjusted to 6 with HCl to increase its solubility (Babić et al. 2006) and stored in refrigerator at -4 ºC in the dark. Samples were mixed in tri-distilled water (10 mg/mL of Enrofloxacin and Oxytetracycline standards reagent grade Sigma-Aldrich, St, Louis, MO, USA) for removal treatments (Du et al. 2017, Esfahani et al. 2019).

Presence of ENRO and OTC in water

The concentration of ENRO and OTC in the model water samples was determined by a method (Babić et al. 2006) of high-performance liquid chromatography/diode array detector (HPLC/DAD) using HPLC/DAD Perkin Elmer (Flexar PDA Plus Detector, Shelton, CT, USA) and the Chromera software version 4.2.0.6415. The column (Spheri-5 RP-18 5 µM 250x4.5 mm, Perkin Elmer, USA) temperature was set to 30 ºC and the injection volume was 20 µL. The mobile phase consisted of a binary mixture of solvents (A: 0.01 M oxalic acid and B: acetonitrile).

The elution started with 100% of A which was maintained for 6 min, followed by 19 min linear gradient to 50% of B and 5 min linear gradient back to 100% of A. Flow rate gradient started with 1.0 mL/min maintained for 6 min, followed by 19 min linear gradient to 0.8 mL/min, and 5 min linear gradient back to 1.0 mL/min. A 30 min post time allowed re-equilibration of the column. Linearity limit of detection (LOD) for ENRO was (0.1 µg/L) and for OTC (10 µg/L), limit of quantification (LOQ) for ENRO was (1.5 µg/L) and for OTC (30 µg/L), recovery was evaluated for quantitative purposes. Calibration

curves were prepared from standard solutions of ENRO and OTC, to calculate the recovery of these antibiotics from the respective solutions before and after removal treatments.

The linearity was evaluated for both ENRO and OTC in the mixture using four concentrations in the range 3.625-25 mg/mL for ENRO, and 0.625-5 mg/mL for OTC. The results were subjected to linear regression analysis to obtain the respective standard equations for Pearson correlation (r) for both drugs (r = 0.9991 for ENRO and r = 0.9992 for OTC) to estimate the ENRO and OTC concentration in the samples and confirm the linearity of the method.

The estimation of the antibiotic concentration in the samples of prepared water of each treatment was made by an external standard method, with the commercial references of ENRO and OTC, by area measurements, using standard curves. Removal treatments were made by preparing 1 L of water and ENRO (10 mg/mL) and 4 g of biocomposite, that was put in constant agitation at 100 rpm during different contact times (0, 2, 6 and 24 h) at pH 6 and temperature of 30 ºC. For samples with OTC, the same operating conditions were maintained, only at pH 7.

The removal percentage (% R) of both antibiotics was calculated using the equation 1 with the data of the initial concentration of the drug Ci (mg/mL) and the final concentration Cf (mg/mL), calculated after each treatment (Jiménez et al. 2017).

$$\% R = \frac{c_i - c_F}{c_i} \times 100 \quad (1)$$

Data analysis

The assays were carried out for three independent subsamples (triplicate) of each sample. Data were subjected to an analysis of variance ($p < 0.05$) and means were separated by the Tukey test.

RESULTS AND DISCUSSION

Characterization of AC and chitosan

Different temperatures, times, and H3PO4 impregnation ratio (0.6 w/v) were assayed to obtain the AC. Treatments 1-5 conditions had an incomplete carbonization because the activation temperatures were not high enough. These results agree with Neolaka et al. (2023), who reported that temperatures above 400 ºC are required to carbonize some materials. For this reason, the products from treatments 1-5 were discarded for further analysis. ACs from bamboo (Suhaimi et al. 2020) and sugar cane bagasse (Chatterjee et al. 2020) obtained at 500 ºC drastically increased their adsorption performances, which were references to select the product of treatment 6 of the current study.

AC with high carbon content and lower ash level (not more than 7% w for the last) are considered suitable as adsorbent material because high ash contents are related to the blocking of the contact surface and porosity of ACs (Mariah et al. 2023). Due to treatments 7-10 showing the highest ash content (7.3-9.7% w/w), they were discarded for further analysis. Treatment 6 (CA6) had a total yield of 22.85% (w/w) of AC, similar to that reported by Neme et al. (2022) of 6-19% (w/w) obtained from castor seed hull. AC from treatment 6 (500 ºC, IR 0.6, 60 min) was selected to prepare the biocomposites, as it represented the highest carbonization (average yield of 22.85% w/w) and the lowest ash content (6.9% w/w).

The time required to prepare AC was the same than reported (60 min) by Abdel-Ghani et al. (2016) from olive tree residues. The impregnation ratio (IR) of treatment 6 was 0.6% H_3PO_4 (w/v) and the average yield obtained (28% w/w) were similar to those reported by Neme et al. (2022), who prepared AC from Castor seed hull (IR = 0.8 H_3PO_4 w/v, 18-24% average yield). Other studies showed a yield of 30.2% for AC obtained from *Cassava* stem at temperatures 450-900 ºC for 150 min under of its own combustion gas (Sulaiman et al. 2018). Yield values of 35% were found for AC synthetized from sunflowers under a N_2 environment at 600 ºC for 150 min (Zhao et al. 203), which represents more drastic conditions than those used in the present study. Synthesis of AC from *Acacia* reported by Gulfam Alam et al. (2023) required a higher temperature (900 ºC) than the required in the current study, but less time of pyrolysis (45 min); however, these authors reported no data for the IR and yield, so no comparison can be done.

The contents of C_2 (46%) and N_2 (0.37%) in the AC selected are shown in **table I**. The values are similar to those reported in the AC from the agave bagasse generated from the tequila production (45%

TABLE I. CARBON (C_2) AND NITROGEN (N_2) PRESENT IN ACTIVATED CARBON (AC) AND COMMERCIAL CHITOSAN.

Sample	C_2 (%)	N_2 (%)
AC	46.54 ± 0.20 a	0.37 ± 0.02 a
Commercial chitosan	37.43 ± 0.2 b	7.22 ± 0.15 b

Different letters in the same column mean significant differences according to the Tukey test ($p < 0.05$).

and 0.3%, respectively), pine wood (48% and 0.01%, respectively), sugar cane bagasse (45.5% and 0.1%, respectively) by Nieto-Delgado (2011). However, the values were lower than those reported for the AC from *Eucalyptus* (48% and 0.5%, respectively) by Heidari et al. (2014) and also lower than those reported for AC from Durian shell (60% and 3%, respectively) reported by Chandra (2009). Many biomasses contain different elemental compositions depending on their nature and the pretreatments used.

The content of C2 found here for chitosan agrees with the content reported for commercial shrimp chitosan (39.2%) by Padilla-Quintero et al. (2017). In contrast, the content of N2 was similar to 7% found for commercial chitosan by Rodríguez-Pedrozo et al. (2009) but less than (40% of C2 and similar at 7.2% N2) found by (Muñoz et al. 2023). The amount of C2 and N2 is related to the deacetylation degree and the number of amine groups available that determine the reactivity and adsorption power of chitosan (Muñoz et al. 2023). This group type can potentially adsorb anions by electrostatic attraction (Sharififard et al. 2012).

Scanning electron microscopy (SEM)

The SEM images of the AC particles at different magnification levels are shown in **figure 1**. The images of electrons reveal the presence of a porous matrix constituted by organic matter, observed by atomic contrast. Macro, meso, and micro porosities were observed, openings and hollow structures were also observed. If activation temperature is higher than 600 ºC, irregularity in shape and size of pore increases (Yorgun et al. 2015).

Microporosity is a sought attribute because it indicates efficacy during the synthesis and activation process; the high formation of microporosity in ACs is related to an increase in efficiency because the available contact surface increases (Sizirici et al. 2021). Another way to increase the surface is by decreasing the size of the AC particle (Saman et al. 2018). These changes occur during physical and chemical treatments during carbonization, as Thileep Kumar et al. (2018) reported.

The control of the H_3PO_4 impregnation ratio maintained a relationship with the amount and heterogeneous porosity size and agreed with the waste

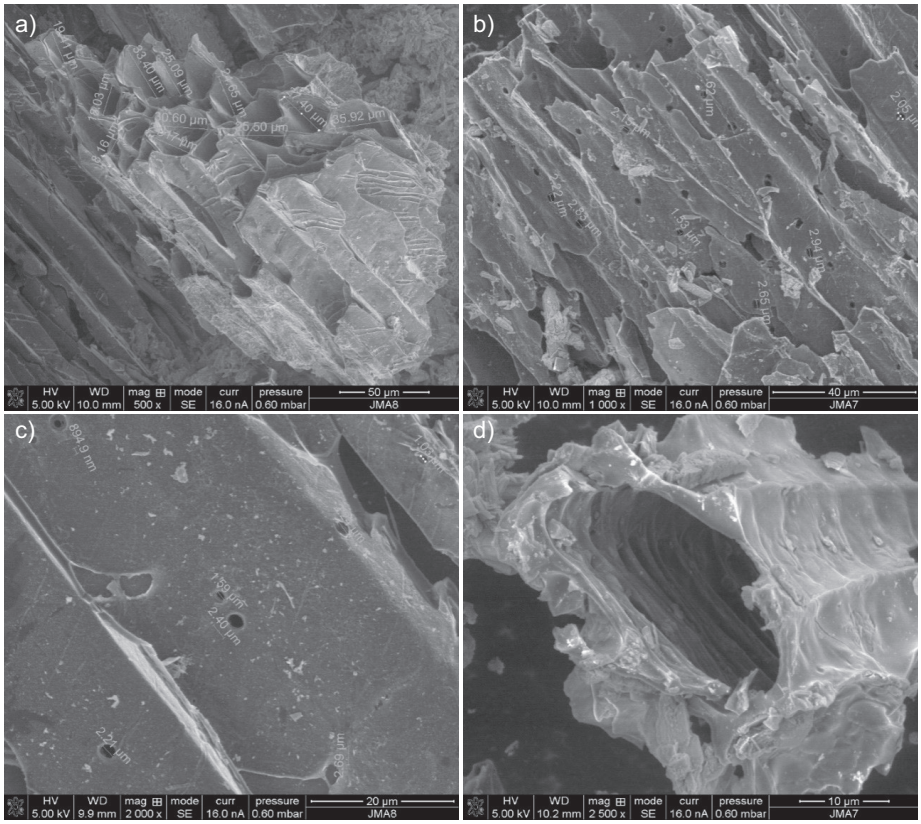

Fig. 1. Scanning electron microscope (SEM) micrographs of the activated carbon (AC) particles (**Table I**) at a: 500X, b:1000X, c: 2000X, d:2500X.

tea AC reported by Mariana et al. (2023). Chemical activators (such as H_3PO_4) contribute to thermal decomposition and increase the amount of porosity present in the carbonized material (Gómez-Delgado et al. 2022). The quantity and pore size are related to the impregnation ratio of the activator agent, which agrees with the reported by Lim et al. (2010) for palm shell AC.

Nanometric grinding

The average size (time 0) found for the AC, as revealed by a DLS analysis, was 31.12 µm. This size contrasted with the obtained after two h of grinding (time 1), which was 1.28 µm, as revealed by the respective DLS analysis. The average size obtained after four h (time 2) was 0.57 µm. Bassyouni et al. (2019) state that particles between 1 nm and 0.1 µm are considered nanoparticles. Thus, after four hours of grinding, AC acquired the condition of a nanoparticle.

AC is frequently used as a standard filler in the preparation of biocomposites due to its physical and chemical properties, which are considered to improve mechanical properties (Rahmi et al. 2018).

According to Kwiatkowski et al. (2022), molecules containing N_2 atoms will not be retained by macro, meso, or microporosities due to kinetic size restrictions of the material. For these reasons, the AC was prepared to nanometric scale and added in the matrix of chitosan.

Biocomposites of chitosan and AC

The success of gelation is related to the degree of deacetylation and molecular weight of chitosan, having a more significant number of amino groups in acid solution due to a higher molecular weight, increasing the number of positive charges (Rodríguez et al. 2010). The increase could have produced a high degree of crosslinking with the AC, as observed in the SEM images of the different synthesized biocomposites, as shown in **figure 2**. There is a relationship between decreasing the quantity and size of pores in chitosan biocomposite particles after adding nanometric scale compounds, so it is essential to control the addition of said materials. An adequate balance allows for obtaining a biocomposite with greater removal efficiency (Al-Salman et al. 2023).

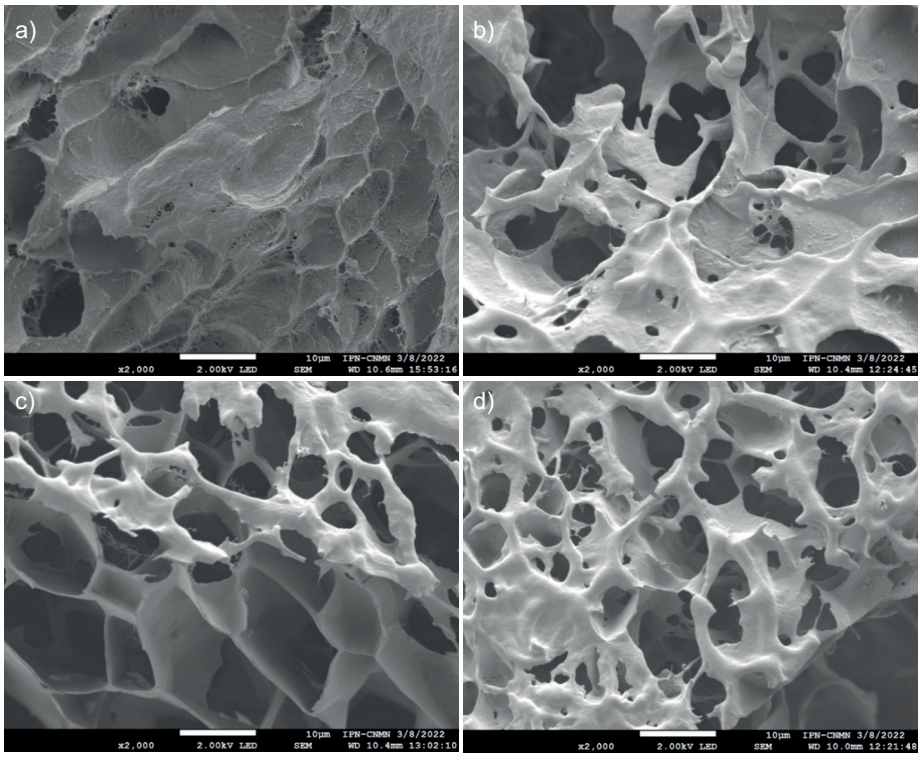

Fig. 2. Scanning electron microscope (SEM) images of the gelation process of chitosan biocomposites at different concentrations of activated carbon (AC): a: 0, b: 0.5, c: 2, d: 5% (w/w).

Physical and chemical characterization

Table II shows the pH values registered for the different biocomposites prepared with chitosan mixed with different amounts (0, 0.5, 2, and 5% w/w) of AC. The electrical conductivity values ranged from 0.331 to 0.387 S/m. These electrical conductivity values can be attributed to the 2% acetic acid content in the medium, which releases H^+, and were higher than those reported by Padilla-Quintero et al. (2017) for a chitosan-glutaraldehyde gel (0.203-0.256 S/m). According to Esfahani et al. (2019) the formation of sponge structures within the biocomposite of chitosan and AC is due to the addition of acid during the gelation process, increasing the number of negative charges of the biocomposite surface, which increases the adsorption capacity of chemical species.

TABLE II. PHYSICAL AND CHEMICAL CHARACTERIZATION OF BIOCOMPOSITES OBTAINED WITH ACTIVATED CARBON (AC) AND CHITOSAN.

Biocomposites containing different amounts AC (%, w/w)	pH	Conductivity (S/m)
0.0	3.5	0.331
0.5	3.5	0.355
2.0	3.7	0.366
5.0	4.0	0.387

Fourier transform infrared spectroscopy (FTIR)

Figure 3 shows the infrared spectra of biocomposites formed with different concentrations of AC (0, 0.5, 2, and 5% w/w) and chitosan. It was possible to identify characteristic functional groups and bands for the AC and the biocomposites formed with the chitosan.

The signals in the spectral region 3700 cm^{-1} correspond to the stretching vibrations of the OH bonds (Morales-Olán et al. 2021). Another band around 1626 cm^{-1} responds to the stretching vibration C=O bond (Luo et al. 2010). The signal at 1562 cm^{-1} represents the bending vibration of the NH bond (Barbosa et al. 2019). The vibration in 1372 cm^{-1} arises from the stretching NH_2 bond (Mauricio-Sánchez et al. 2018). The vibration in 1370 cm^{-1} is related to the stretching and symmetrical deformation in the CH_3 bond (Branca et al. 2016). Fingerprint bands were between 1500-900 cm^{-1}, which were helpful in evidencing chitosan presence. The little peak at the region of 1146 cm^{-1} is assigned to the stretching of CO (Corazzari et al. 2015). Another band at 1058 cm^{-1} corresponds to the stretching vibration of the P-O-P bond, reported by Neme et al. (2022). The vibration peak in the frequency 1028 cm^{-1} corresponds to the stretching C=C of the aromatic ring (Wibawa et al. 2020). The absorption band at 888 cm^{-1} is related to the stretching vibration of the C-O-C bond characteristic in the union between AC and chitosan, as described by (Rahmi et al. 2018). The

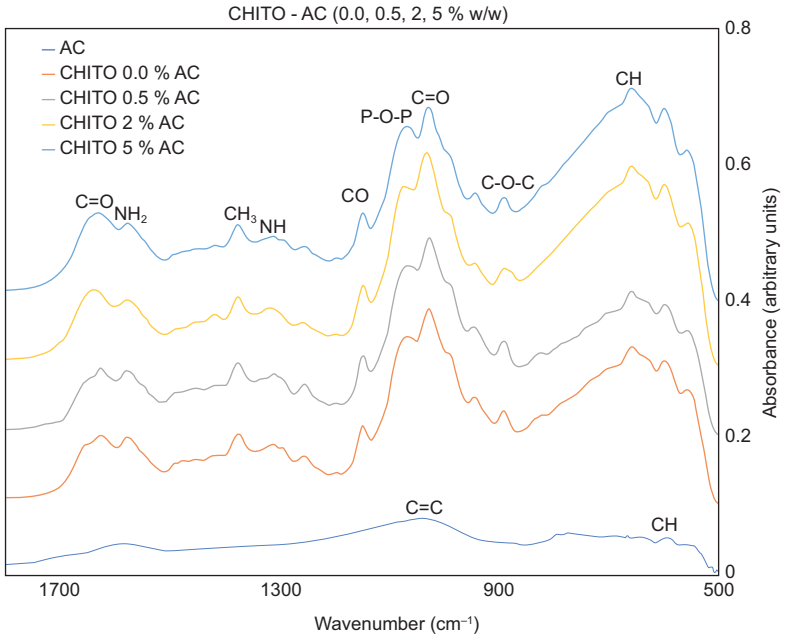

Fig. 3. Fourier transform infrared spectroscopy (FTIR) spectra of biocomposites formed of chitosan (CHITO) with several amounts of activated carbon (AC): 0% AC, 0.5% AC, 2% AC, 5% AC (w/w).

peak in the region 656 cm^{-1} is attributed to the CH stretching (Cui et al. 2021). Finally, the absorption band at 584 cm^{-1} corresponds to the CH_3 binding in activated carbons (Mariana et al. 2023).

This vibrational characterization indicated that the nanoparticles of AC were attached to the chitosan biocomposite, and a stable chemical crosslink was formed during the polymerization process. The functional groups of each material were preserved after the polymerization process according to what Ang et al. (2019) described, improving the ability to bind with other molecules according to what was described by Kumar et al. (2019).

Presence of ENRO and OTC in water

Separation and identification of both drugs were done using the method proposed in this work. The HPLC chromatograms of ENRO and OTC are shown in **figures 4a** and **4b**, respectively. The retention times for the drugs were 25 min for ENRO, which agreed with reported by Babić et al. (2006), and 21 min for OTC, a lower value than 25.9 reported by Sanderson et al. (2005). The values found for the removal of drugs at times of 0, 2, 6, and 24 h are shown in **table III** and **IV**. The values found for the removal of drugs at different times (0, 2, 6, and 24 h) are shown in **figures 5** and **6**. A concentration of 10 mg/mL (10 000 ppm) was based on other contaminants removal biocomposites studies, where 100 000 ppm concentration was used (Esfahani et al. 2019).

The removal capacity was dependent on both AC biocomposite concentration and time. Our results, which are consistent with those of Wu et al. (2021), underscore the importance of time increments in improving removal capacity. However, it's crucial to note that after more than an hour, the adsorption ability can decrease due to the reduction of functional groups on the surface of the biocomposite. Our study, in comparison to existing research on the treatment and removal of ENRO and OTC, demonstrates the adsorption capacities of different biocomposites under various operating conditions. For instance, grafted chitosan hydrogel in water with an ENRO concentration of 600 mg/L showed a removal capacity of 388 mg/g (Karmi-Maleh et al. 2021), which is in line with our study's findings.

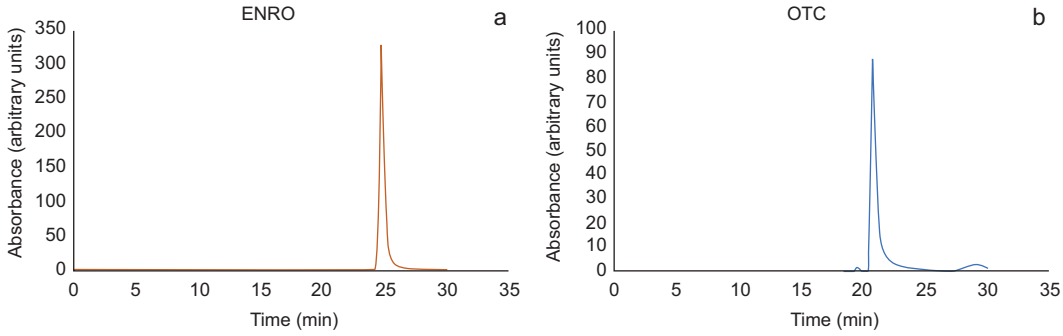

Fig. 4. High-performance liquid chromatography-diode array detector (HPLC-DAD) chromatograms of a: enrofloxacin (ENRO), and b: oxytetracycline (OTC) standard solutions.

TABLE III. REMOVAL PERCENTAGES (%R) OF ENROFLOXACIN (ENRO) FROM AN AQUEOUS SOLUTION (10 mg/mL) WITH THE DIFFERENT CHITOSAN (CHITO) AND ACTIVATED CARBON (AC) BIOCOMPOSITES AFTER DIFFERENT CONTACT TIMES (0, 2, 6, 24 h).

Biocomposites containing different amount of AC (%, w/w)	%R (0 h)	%R (2 h)	%R (6 h)	%R (24 h)
CHITO / 0.0% AC	0	25.66 ± 0.5 a	27.60 ± 1.4 a	28.33 ± 1.5 a
CHITO / 0.5% AC	0	34.33 ± 1.5 a	39.66 ± 1.5 b	40.31 ± 2.0 b
CHITO / 2% AC	0	40.33 ± 1.5 b	48.66 ± 1.1 c	50.30 ± 2.0 c
CHITO / 5% AC	0	45.44 ± 1.1 b	49.37 ± 2.0 c	48.66 ± 0.5 c

Different letters in the same column mean significant differences according to the Tukey test ($p < 0.05$).

TABLE IV. REMOVAL PERCENTAGES (%R) OF OXYTETRACYCLINE (OTC) FROM AQUEOUS SOLUTION (10 mg/mL) WITH THE DIFFERENT CHITOSAN (CHITO) AND ACTIVATED CARBON (AC) BIOCOMPOSITES AFTER DIFFERENT CONTACT TIMES (0, 2, 6, 24 h).

Biocomposites containing different amount of AC (%, w/w)	%R (0 h)	%R (2 h)	%R (6 h)	%R (24 h)
CHITO / 0.0% AC	0	40.33 ± 0.5 a	41.19 ± 1.1 a	44.54 ± 1.2 a
CHITO / 0.5% AC	0	50.11 ± 2.6 b	56.49 ± 1.0 b	59.38 ± 1.0 b
CHITO / 2% AC	0	56.66 ± 1.5 c	53.22 ± 1.0 b	54.62 ± 1.5 a
CHITO / 5% AC	0	57.05 ± 1.0 c	57.66 ± 1.1 c	58.33 ± 1.5 c

Different letters in the same column mean significant differences according to the Tukey test ($p < 0.05$).

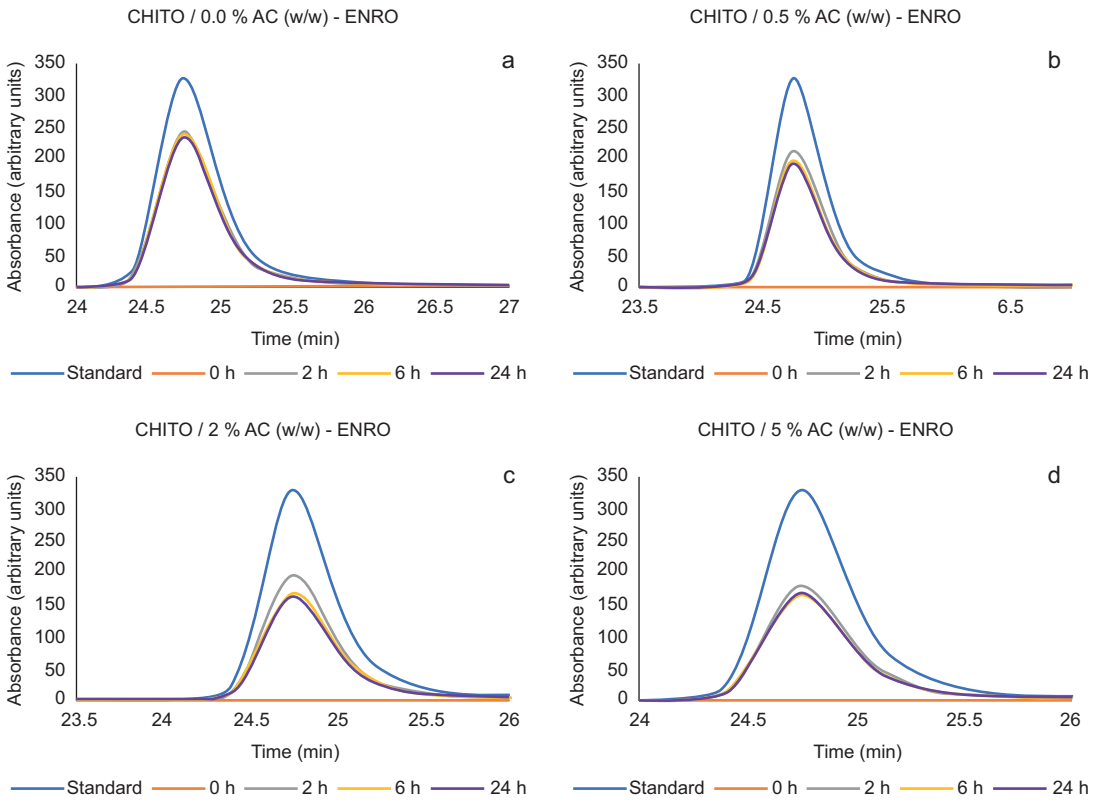

Fig. 5. High-performance liquid chromatography-diode array detector (HPLC-DAD) chromatograms of removal treatments of enrofloxacin (ENRO) in aqueous solution (10 mg/mL) with the different chitosan (CHITO) and activated carbon (AC) biocomposites. a: CHITO / 0.0% AC, b: CHITO / 0.5% AC, c: CHITO / 2% AC, and d: CHITO / 5% AC (w/w) at different contact times (0, 2, 6, and 24 h).

Studies based on ZSM nanosized zeolite–carbon composite showed an adsorption capacity of 88 mg/g of adsorbate, a low performance due to the low affinity of the adsorbent material with the drug (Al-Jubouri et al. 2022). To remove OTC, reduced graphene oxide nanocomposites have been used at a concentration of 600 mg/L of OTC solved in water with a removal capacity of 177 mg/g of adsorbent. It was shown that the adsorption of biocomposites of chitosan and AC performed better (Hao et al. 2021). Nanocomposite formed by Zeolite/Fe_3O_4 showed an adsorption capacity of 83 mg/g adsorbate in a

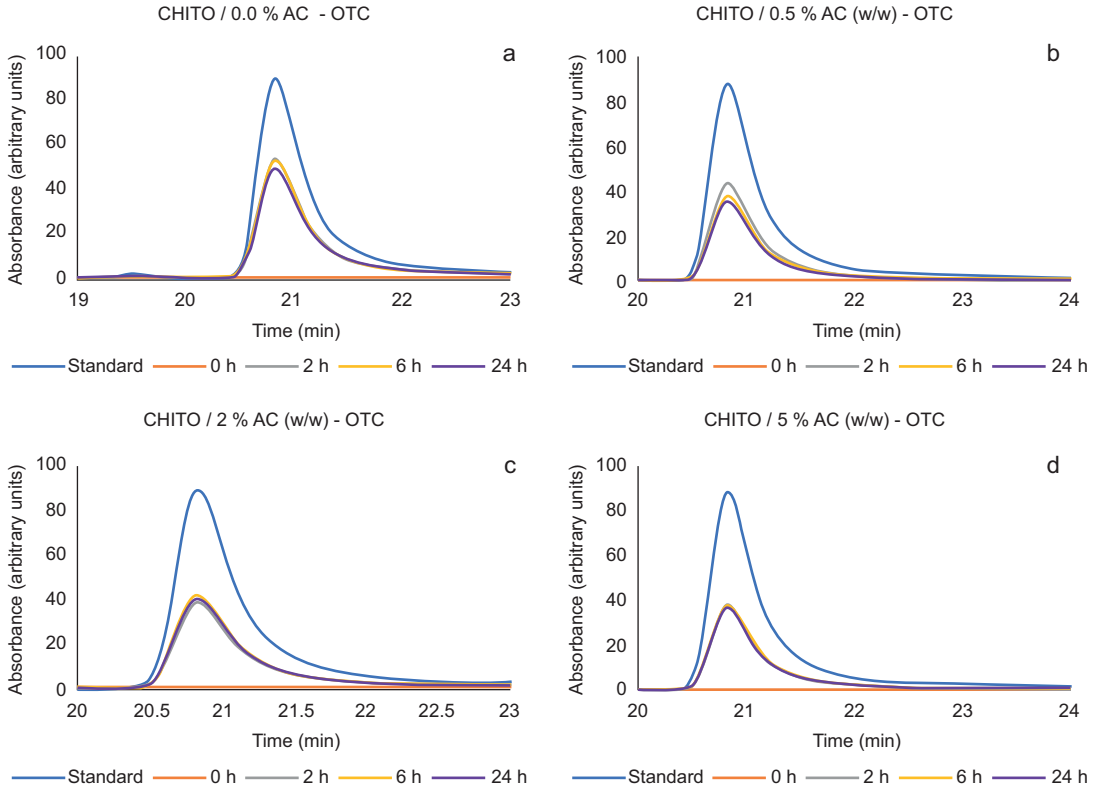

Fig. 6. High-performance liquid chromatography-diode array detector (HPLC-DAD) chromatograms of removal treatments of oxytetracycline (OTC) in aqueous solution (10 mg/mL) with the different chitosan (CHITO) and activated carbon (AC) biocomposites. a: CHITO / 0.0% AC (w/w), b: CHTO / 0.5% AC, c: CHITO / 2% AC, and d: CHITO / 5% AC (w/w) at different contact times (0, 2, 6, and 24 h).

solution of OTC in water, less than other treatments (Baskan et al. 2022). Studies carried out with BiO_2/BiOCl composites supported on graphene-chitosan and photocatalysis showed a 63% OTC removal capacity (Priya et al. 2016).

The results for removal capacity for different drugs by a composite with nanometric scale material is 500-900 mg/g of adsorbent material in low-concentration solutions (12 mg/L). This capacity is more significant than each component separately (Nayak et al. 2023).

There are other biocomposites or nanocomposites that have been manufactured with different materials and whose removal capacity is function of materials which biocomposite was synthetized and affinity with contaminant to be removed. Some of these materials and their removal capacity are magnetic CS nanoparticles (27.5 mg/g of adsorbent), glutaraldehyde crosslinked CS (180 mg/g) for removal heavy metals (Chang et al. 2006), MWCNT-PDA-CS-GO (150 mg/g) of Li removal (Zhang et al. 2021), and magnetic crosslinked CS (171 mg/g) for removal Pt (IV) from water (Zhou et al. 2010).

The performance of biocomposites also depends on drug concentration and its affinity with the adsorbent (Li et al. 2021). A greater removal capacity of AC is due to a higher electron density in the planes of aromatic rings, establishing H2 bridges between OH- groups of the oxytetracycline and the oxygenated groups of carbon. Saturation of porosities and active sites of biocomposite particles can produce blockages, decreasing efficiency by reducing the available surface area. To avoid this problem, washing, recovery, and reuse treatments are necessary (Rivera et al. 2013).

Some reports suggest that waste from antibiotic-treated animals can be composted, resulting in drug degradation in approximately 30 days (Arikan et al. 2009). In this study, we propose a scheme that could be tested once the antibiotics are captured and concentrated in the biocomposite. The use of these

biocomposites represent a good option due to low cost to obtain a raw material. However, it's crucial to emphasize the need for further systematic studies on the effect of AC-chitosan biocomposites to optimize performance and efficiency of drug removal, implementing variations in parameters such as pH, temperature and pressure that could increase the percentage of drug removal, taking into account the price–performance ratio.

AC particle type with specific physical and chemical properties (surface charge, composition, contact surface) and amount of chitosan can improve the performance of biocomposites in other water treatment processes, such as desalination, removal of drugs, heavy metals, and organic and inorganic contaminants.

CONCLUSIONS

The synthesis conditions (500 ºC, IR 0.6, 60 min) allowed to obtain, after grinding, 571 nm AC particles.

The addition of AC to the chitosan formed a biocomposite with high porosity. The characteristic functional groups observed by FTIR spectroscopy on AC and the chitosan biocomposites suggest that the nanoparticles of AC were attached to the chitosan biocomposite, and a stable chemical crosslinking was formed during the polymerization process.

The results showed that the addition of AC to chitosan formed a biocomposite with the capacity to remove 59.3% of OTC (contact time two h at 100 rpm, 4 g biocomposite/L solution, pH 6-7, 30 ºC) and, in a lower percentage, 50.3% of ENRO (contact time two h at 100 rpm, 4 g biocomposite/L solution, pH 6, 30 ºC).

The AC and chitosan biocomposite synthesis method is simple, fast, and degradable. The continuum development of techniques for synthesizing biocomposites will provide new knowledge on the objects under investigation.

REFERENCES

Abdel-Ghani N.T., El-Chaghabi G.A., ElGammal M.H. and Rawash E.-S.A. (2016). Optimizing the preparation conditions of activated carbons from olive cake using KOH activation. New Carbon Materials 31 (5), 492-500. https://doi.org/10.1016/S1872-5805(16)60027-6

Alanazi F., Almugbel R., Maher H.M., Alodaib F.M. and Alzoman N.Z. (2021). Determination of tetracycline, oxytetracycline and chlortetracycline residues in seafood products of Saudi Arabia using high performance liquid chromatography-photo diode array detection. Saudi Pharmaceutical Journal 29 (6), 566-575. https://doi.org/10.1016/j.jsps.2021.04.017

Al-Jubouri S.M., Al-Jendeel H.A., Rashid S.A. and Al-Batty S. (2022). Antibiotics adsorption from contaminated water by composites of ZSM-5 zeolite nanocrystals coated carbon. Journal of Water Process Engineering 47, 122745. https://doi.org/10.1016/j.jwpe.2022.102745

Al-Salman H.N.K., Falih M., Deab H.B., Altimari U.S., Shakier H.G., Dawood A.H., Ramadan M.F., Mahmud Z.H., Farhan M.A., KÖten H. and Kianfar E. (2023). A study in analytical chemistry of adsorption of heavy metal ions using chitosan/graphene nanocomposites. Cases Studies in Chemical and Environmental Engineering 8, 1004026. https://doi.org/10.1016/j.cscee.2023.100426

Ang M.B., Ji Y.-L., Huang S.-H., Lee K.-R. and Lai J.-Y. (2019). A facile and versatile strategy for fabricating thin-film nanocomposite membranes with polydopamine-piperazine nanoparticles generated in situ. Journal of Membrane Science 579, 79-89. https://doi.org/10.1016/j.memsci.2019.02.064

Anita S., Hanifah T.A., Itanwita. and Kartika G.F. (2023). Preparation and characterization of activated carbon from the nipa fruit shell irradiated by microwave: Effect temperatures and time of carbonization. Materials Today: Proceedings 87 (2), 390-395. https://doi.org/10.1016/j.matpr.2023.04.172

AOAC (2010). Official methods of analysis. Microchemical determination of nitrogen. Micro-Kjeldahl method. 17th ed, AOAC International, Gaithersburg, Maryland, USA, 2200 pp.

Arikan O., Mulbry W. and Rice C. (2009). Management of antibiotic residues from agricultural sources: Use of composting to reduce chlortetracycline residues in beef manure from treated animals. Journal of Hazardous Materials 164 (2-3), 483-489. https://dx.doi.org/10.1016/j.jhazmat.2008.08.019

Babel S. and Kurniawan T.A. (2003). Low-cost adsorbents for heavy metals uptake from contaminated water: A review. Journal of Hazardous Materials 97 (1-3), 219-243. https://doi.org/10.1016/S0304-3894(02)00263-7

Babić S., Ašperger D., Mutavdžić D., Horvat A.J.M. and Kaštelan-Macan M. (2006). Solid phase extraction and HPLC determination of veterinary pharmaceuticals in wastewater. Talanta 70 (4), 732-738. https://doi.org/10.1016/j.talanta.2006.07.003

Baig M., Ingole P., Jeon J., Hong S., Choi W., Jang B. and Lee H. (2019). Water vapor selective thin film

nanocomposite membranes prepared by functionalized silicon nanoparticles. Desalination 451, 59-71. https://doi.org/10.1016/j.desal.2017.06.005

Barbosa H.F.G., Francisco D.S., Ferreira A.P.G. and Cavalheiro É.T.G. (2019). A new look towards the thermal decomposition of chitins and chitosans with different degrees of deacetylation by coupled TG-FTIR. Carbohydrate Polymers 225, 115232. https://doi.org/10.1016/j.carbpol.2019.115232

Baskan G., Acikel U. and Levent M. (2022). Investigation of adsorption properties of oxytetracycline hydrochloride on magnetic zeolite/Fe_3O_4 particles. Advanced Powder Technology 33 (6), 103600. https://doi.org/10.1016/j.apt.2022.103600

Bassyouni M., Abdel-Aziz M., Zoromba M., Abdel-Hamid S. and Drioli E. (2019). A review of polymeric nanocomposite membrane with enhanced permeation, rejection and self-cleaning ability. Journal of Industrial and Engineering Chemistry 73, 19-46. https://doi.org/10.1016/j.jiec.2019.01.045

Benedetti V., Patuzzi F. and Baratieri M. (2017). Characterization of char from biomass gasification and its similarities with activated carbon in adsorption applications. Applied Energy 227, 92-99. http://dx.doi.org/10.1016/j.apenergy.2017.08.076

Betancourt-Galindo R., Reyes-Rodríguez P., Puente-Urbina B., Ávila-Orta C., Rodríguez-Fernández O. and Cárdenas-Pliego G. (2014). Synthesis of copper nanoparticles by thermal decomposition and their antimicrobial properties. Journal of Nanomaterials 2014, 980545. http://doi.org/10.1155/2014/980545

Branca C., D'Angelo G., Cupri C., Khouzami K., Rifici S., Ruello G. and Wanderlingh H. (2016). Role of the OH and NH vibrational groups in polysaccharide-nanocomposite interactions: A FT-IR-ATR study on chitosan and chitosan/clay films. Polymer 99, 614-622. http://dx.doi.org/10.1016/j.polymer.2016.07.086

Chandra T.C., Mirna M.M., Sunarso J., Sudaryanto Y. and Ismadji S. (2009). Activated carbon from durian shell: Preparation and characterization. Journal of the Taiwan Institute of Chemical Engineers 40 (4), 457-462. https://doi.org/10.1016/j.jtice.2008.10.002

Chang Y.C., Chang S.W. and Cheng D.H. (2006). Magnetic chitosan nanoparticles: Studies on chitosan binding and adsorption of Co (II) ions. Reactive and Functional Polymers 66 (3), 335-341. https://doi.org/10.1016/j.reactfunctpolym.2005.08.006

Chatterjee R., Sajjadi B. and Chen W.Y. (2020). Effect of pyrolysis temperature on physicochemical properties and acoustic-based amination of biochar for efficient CO_2 Adsorption. Frontiers in Energy Research 8, 85. https://doi.org/10.3389/fenrg.2020.00085

Corazzari I., Nisticò R., Turci F., Faga M. G., Franzoso F., Tabasso S. and Magnacca G. (2015). Advanced physico-chemical characterization of chitosan by means of TGA coupled on-line with FTIR and GCMS: Thermal degradation and water adsorption capacity. Polymer Degradation and Stability 112, 1-9. https://doi.org/10.1016/j.polymdegradstab.2014.12.006

Cui F., Li H., Chen C., Wang Z., Liu X., Jiang G., Cheng T., Bai R. and Song L. (2021). Cattail fibers as source of cellulose to prepare a novel type of composite aerogel adsorbent for the removal enrofloxacin in wastewater. International Journal of Biological Macromolecules 191, 171-181. https://doi.org/10.1016/j.ijbiomac.2021.09.022

Daniel L.S., Rahman A., Hamushembe M.N., Kapolo P., Uahengo V. and Jonnalagadda S.B. (2023). The production of activated carbon from *Acacia erioloba* seedpods via phosphoric acid activation method for the removal of methylene blue from water. Bioresource Technology Reports 23, 101568. https://doi.org/10.1016/j.biteb.2023.101568

Dilekoglu M.F. and Yapici M. (2023). Adsorption of naproxen pharmaceutical micropollutant from aqueous solutions on superior activated carbon synthetized from sheep manure: Kinetics, thermodynamics, and mechanism. Journal of Molecular Liquids 381, 121839. https://doi.org/10.1016/j.molliq.2023.121839

Dizbay-Onat M., Vaidya U. and Lungu C.T. (2017). Preparation of industrial sisal fiber waste derived activated carbon by chemical activation and effects of carbonization parameters on surface characteristics. Industrial Crops and Products 95, 583-590. https://doi.org/10.1016/j.indcrop.2016.11.016

Du J., Zhao H., Liu S., Xie H., Wang Y. and Chen J. (2017). Antibiotics in the coastal water of the South Yellow Sea in China: Occurrence, distribution and ecological risks. Science of the Total Environment 595, 521-527. http://dx.doi.org/10.1016/j.scitotenv.2017.03.281

Esfahani M.R., Koutahzadeh N., Esfahani A.R., Firouzjaei M.D., Anderson B. and Peck L. (2019). A novel gold nanocomposite membrane with enhance permeation, rejection and self-cleaning ability. Journal of Membrane Science 573, 309-319. https://doi.org/10.1016/j.memsci.2018.11.061

Fathizadeh M., Tien H., Khivantsev K., Song Z., Zhou F. and Yu M. (2019). Polyamide/nitrogen-doped graphene oxide quantum dots (N-GOQD) thin-film nanocomposite reverse osmosis membranes for high flux desalination. Desalination 451, 125-132. https://doi.org/10.1016/j.desal.2017.07.014

Gomez-Delgado E., Nunell G., Cukierman A. L. and Bonelli P. (2022). Agroindustrial waste conversion

into ultramicroporous activated carbons for greenhouse gases adsorption-based processes. Bioresource Technology Reports 18, 101008. https://doi.org/10.1016/j.biteb.2022.101008

González-García P. (2018). Activated carbon from lignocellulosic precursors: A review of synthesis methods, characterization techniques, and applications. Renewable and Sustainable Energy Reviews 82 (1), 1393-1414. https://doi.org/10.1016/j.rser.2017.04.117

Guerrero-Pérez M., Valero-Romero M., Hernández S., Nieto J., Rodríguez-Mirasol J. and Cordero T. (2012). Lignocellulosic-derived mesoporous materials: An answer to manufacturing non-expensive catalysis useful for the biorefinery processes. Catalysis Today 195 (1), 155-161. http://doi.org/10.1016/j.cattod.2012.03.068

Gulfam Alam M., Danish M., Alanazi A.M., Ahmad T. and Abdul Khalil H.P.S. (2023). Response surface methodology approach of phenol removal study using high-quality activated carbon derived from H_3PO_4 activation of *Acacia mangium* wood. Diamond and Related Materials 132, 109632. https://doi.org/10.1016/j.diamond.2022.109632

Hao D., Song Y.-X., Zhang Y. and Fan H.-T. (2021). Nanocomposites of reduced graphene oxide with pure monoclinic–ZrO_2 and pure tetragonal–ZrO_2 for selective adsorptive removal of oxytetracycline. Applied Surface Science 543, 148810. https://doi.org/10.1016/j.apsusc.2020.148810

Heidari A., Younesi H., Rashidi A. and Ghoreyshi A. (2014). Adsorptive removal of CO_2 on highly microporous activated carbons prepared from *Eucalyptus camaldulensis* wood: Effect of chemical activation. Journal of the Taiwan Institute of Chemical Engineers 45 (2), 579-588. https://doi.org/10.1016/j.jtice.2013.06.007

Hussain O.A., Hathout A.S., Abdel-Mobdy Y.E., Rashed M.M., Abdel Rahim E.A. and Fouzy A.S.M. (2023). Preparation and characterization of activated carbon from agricultural wastes and their ability to remove chlorpyrifos from water. Toxicology Reports 10, 146-154. https://doi.org/10.1016/j.toxrep.2023.01.011

Jiménez Ramos I., Rondón W., Rojas de Astudillo L., Rojas de Gáscue B., Prin J. L., Freire D., Díaz I., Pino K. and González O. (2017). Síntesis de carbón activado a partir de epicarpio de *Attalea macrolepis* y su aplicación en la remoción de Pb^{2+} en soluciones acuosas. Revista Internacional de Contaminación Ambiental 33 (2), 303-316. https://doi.org/10.20937/RICA.2017.33.02.11

Karmi-Maleh H., Ayati A., Davoodi R., Tanhaei B., Karimi F., Malekmohammadi S. and Sillampää M. (2021). Recent advances in using of chitosan-based adsorbents for removal of pharmaceutical contaminants: A review. Journal of Cleaner Production 291, 125880. https://doi.org/10.1016/j.jclepro.2021.125880

Kulkarni S. (2015). Nanotechnology: principles and practices. 3rd ed. Springer International Publishing, New York, USA, 418 pp.

Kumar M., RaoT S., Isloor A.M., Ibrahim G.P.S., Inamuddin, Ismail N., Ismail A.F. and Asiri A.M. (2019). Use of cellulose acetate/polyphenylsulfone derivatives to fabricate ultrafiltration hollow fiber membranes for the removal of arsenic from drinking water. International Journal of Biological Macromolecules 129, 715-727. https://doi.org/10.1016/j.ijbiomac.2019.02.017

Kwiatkowski M., Hu X. and Pastusziński P. (2022). Analysis of the influence of activated carbons production conditions on the porous structure formation on the basis of carbon dioxide adsorption isotherms. Materials 15 (22), 7939. https://doi.org/10.3390/ma15227939

Lewoyehu M. (2021). Comprehensive review on synthesis and application of activated carbon from agricultural residues for the remediation of venomous pollutants in wastewater. Journal of Analytical and Applied Pyrolysis 159, 105279. https://doi.org/10.1016/j.jaap.2021.105279

Li F., Wang M., Zhuo J., Yang M. and Wang T. (2021). Cyclodextrin-derivatized hybrid nanocomposites as novel magnetic solid–phase extraction adsorbent for preconcentration of trace fluoroquinolones from water samples coupled with HPLC-MS/MS determination. Microchemical Journal 164, 105955. https://doi.org/10.1016/j.microc.2021.105955

Lim W.C., Srinivasakannan C. and Balasubramanian N. (2010). Activation of palm shells by phosphoric acid impregnation for high yielding activated carbon. Journal of Analytical and Applied Pyrolysis 88 (2), 181-186. https://doi.org/10.1016/j.jaap.2010.04.004

López-Muñoz H. (2022). Síntesis y aplicación de un nanocomposito de quitosano-glicidil metacrilato-colágeno tipo I y partículas de oro sobre la cicatrización de heridas cutáneas. Ph.D. Thesis. Centro de Investigación y Estudios Avanzados Unidad Zacatenco, Instituto Politécnico Nacional, Mexico City, Mexico, 80 pp.

Luo Y., Zhang B., Cheng W.-H. and Wang Q. (2010). Preparation, characterization and evaluation of selenite loaded chitosan/TPP nanoparticles with or without zein coating. Carbohydrate Polymers 82 (3), 942-951. http://dx.doi.org/10.1016/j.carbpol.2010.06.029

Mariah M.A., Rovina K., Vonnie J.M. and Erna K.H. (2023). Characterization of activated carbon from waste tea (*Camellia sinensis*) using chemical activation for removal of methylene blue and cadmium ions. South African Journal of Chemical Engineering 44, 113-122. https://doi.org/10.1016/j.sajce.2023.01.007

Mariana M., Mistar E.M., Aswita D., Zulkipli A.S. and Alfatha T. (2023). Nipa palm shell as a sustainable

precursor for synthesizing high-performance activated carbon: Characterization and application for Hg^{2+} adsorption. Bioresource Technology Reports 21, 101329. https://doi.org/10.1016/j.biteb.2022.101329

Martín J., Gonkowski S., Kortas A., Sobiech P., Rytel L., Santos J.L., Aparicio I. and Alonso E. (2023). Multiclass method to determine emerging pollutants in bats using a non-invasive approach based on guano matrix. Microchemical Journal 188, 108486. https://doi.org/10.1016/j.microc.2023.108486

Mauricio-Sánchez R.A., Salazar R., Luna-Bárcenas J.G. and Mendoza-Galván A. (2018). FTIR spectroscopy studies on the spontaneous neutralization of chitosan acetate films by moisture conditioning. Vibrational Spectroscopy 94, 1-6. https://doi.org/10.1016/j.vibspec.2017.10.005

Mohamad Zaidi N.A.H., Sallehuddin F.N., Lim L.B.L. and Kooh M.R. (2021). Surface modification of *Artocarpus odoratissimus* leaves using NaOH, SDS and EDTA to enhance adsorption of toxic crystal violet dye. International Journal of Environmental Analytical Chemistry 103 (8), 1836-1854. https://doi.org/10.1080/03067319.2021.1884238

Morales-Olán G., Luna-Suárez S., Figueroa-Cárdenas J.D., Correa M. and Rojas-López M. (2021). Synthesis and characterization of chitosan particles loaded with antioxidants extracted from chia (*Salvia hispánica* L.) seeds. International Journal of Analytical Chemistry 2021, 5540543. https://doi.org/10.1155/2021/5540543

Muñoz-Núñez C., Cuervo-Rodríguez R., Echeverría C., Fernández-García M. and Muñoz-Bonilla A. (2023). Synthesis and characterization of thiazolium chitosan derivative with enhanced antimicrobial properties and its use as component of chitosan-based films. Carbohydrate Polymers 302, 120438. https://doi.org/10.1016/j.carbpol.2022.120438

Nayak A., Bhushan B. and Kotnala S. (2023). Evaluation of hydroxyapatite-chitosan-magnetite nanocomposites for separation of pharmaceuticals from water: A mechanistic and comparative approach. Journal of Hazardous Materials Advances 10, 100308. http://doi.org/10.1016/j.hazadv.2023.100308

Neme I., Gonfa G. and Masi C. (2022). Preparation and characterization of activated carbon from castor seed hull by chemical activation with H_3PO_4. Results in Materials 15, 100304. https://doi.org/10.1016/j.rinma.2022.100304

Neolaka Y.A.B., Riwu A.A.P., Aigbe U.O., Ukhurebor K.E., Onyancha R.B., Darmokoesoemo H. and Kusuma H.S. (2023). Potential of activated carbon from various sources as a low-cost adsorbent to remove heavy metals and synthetic dyes. Results in Chemistry 5, 100711. https://doi.org/10.1016/j.rechem.2022.100711

Nieto-Delgado C., Terrones M. and Rangel-Méndez J.R. (2011). Development of highly microporous activated carbon from the alcoholic beverage industry organic by-products. Biomass and Bioenergy 35 (1), 103-112. https://doi.org/10.1016/j.biombioe.2010.08.025

Nisticò R., Lavagna L., Versaci D., Ivanchenko P. and Benzi P. (2020). Chitosan and its char as fillers in cement-base composites: A case study. Boletín de la Sociedad Española de Cerámica y Vidrio 59 (5), 186-192. https://doi.org/10.1016/j.bsecv.2019.10.002

Padilla-Quintero B., Cardona-Trujillo V., Muñoz G., Lizcano-Valbuena W., Zuluaga F., Giraldo-Parra W. and Rodríguez-Marmolejo A. (2017). Preparación y caracterización de geles coductores a base de quitosano para posibles aplicaciones biomédicas. Revista de Ciencias 21 (1), 91-99. https://doi.org/10.25100/rc.v21i1.6349

Pallarés J., González-Cencerrado A. and Arauzo I. (2018). Production and characterization of activated carbon from barley straw by physical activation with carbon dioxide and steam. Biomass and Bioenergy 115, 64-73. https://doi.org/10.1016/j.biombioe.2018.04.015

Priya B., Raizada P., Singh N., Thakur P. and Singh P. (2016). Adsorptional photocatalytic mineralization of oxytetracycline and ampicillin antibiotics using Bi_2O_3 /BiOCl supported on graphene sand composite and chitosan. Journal of Colloid and Interface Science 479, 271-283. http://doi.org/10.1016/j.jcis.2016.06.067

Rahman N. and Raheem A. (2022). Fabrication of graphene oxide/inulin impregnated with ZnO nanoparticles for efficient removal of enrofloxacin from water: Taguchi-optimized experimental analysis. Journal of Environmental Management 318, 115525. https://doi.org/10.1016/j.jenvman.2022.115525

Rahmi., Lelifajri. and Nurfatimah R. (2018). Preparation of pholyethylene glycol diglycidyl ether (PEDGE) crosslinked chitosan/activated carbon composite film for Cd^{2+} removal. Carbohydrate Polymers 199, 499-505. https://doi.org/10.1016/j.carbpol.2018.07.051

Rivera-Utrilla J., Gómez-Pacheco C.V., Sánchez-Polo M., López-Peñalver J.J. and Ocampo-Pérez R. (2013). Tetracycline removal from water by adsorption/bioadsorption activated carbons and sludge–derived adsorbents. Journal of Environmental Management 131, 16-24. https://doi.org/10.1016/j.jenvman.2013.09.024

Robles E., Fernández-Rodríguez J., Barbosa A., Gordobil O., Carreño N. and Labidi J. (2018). Production of cellulose nanoparticles from blue agave waste treated with environmentally friendly processes. Carbohydrate Polymers 183, 294-302. https://doi.org/10.1016/j.carbpol.2018.01.015

Rodríguez-Hamamura N., Valderrama-Negron A., Alarcón-Cavero H. and López-Milla A. (2010). Preparación

de partículas de quitosano reticuladas con tripolifosfato y modificadas con polietilenglicol. Revista de la Sociedad Química del Perú 76, 340-351.

Rodríguez-Pedroso A.T., Ramírez-Arrebato M.A., Rivero-González D., Bosquez-Molina E., Barrera-Necha L.L. and Bautista-Baños S. (2009). Propiedades químico-estructurales y actividad biológica de la quitosana en microorganismos fitopatógenos. Revista Chapingo Serie Horticultura 15, 307-317.

Saman N., Abdul Aziz A., Johari K., Song S. and Mat H. (2018). Adsorptive efficacy analysis of lignocellulosic waste carbonaceous adsorbents toward different mercury species. Process Safety and Environmental Protection 96, 33-42. https://doi.org/10.1016/j.psep.2015.04.004

Sanderson H., Ingerslev F., Brain R.A., Halling-Sørensen B., Bestari J., Wilson C. J., Johonson D.J. and Solomon K.R. (2005). Dissipation of oxytetracycline, chlortetracycline and doxycycline using HPLC-UV and LC/MS/MS under aquatic semi-field microcosm conditions. Chemosphere 60 (5), 619-629. https://doi.org/10.1016/j.chemosphere.2005.01.035

SEMARNAT (2002). Norma Oficial Mexicana NOM-021-RECNAT-2000. Que establece las especificaciones de fertilidad, salinidad y clasificación, estudio, muestreo y análisis de suelos. Secretaría de Medio Ambiente, Recursos Naturales y Pesca. Diario Oficial de la Federación, Mexico City, Mexico, December 31th 2002.

Sharififard H., Zokaee Asthiani F. and Soleimani M. (2012). Adsorption of palladium and platinum from aqueous solutions by chitosan and activated carbon coated with chitosan. Asia-Pacific Journal of Chemical Engineering 172 (3), 384-395. http://doi.org/10.1002/apj.1671

Sharififard H., Shahraki Z., Rezvanpanah E. and Rad S. (2018). A novel natural chitosan/activated carbon/iron bio-nanocomposite: Sonochemical synthesis, characterization, and application for cadmium removal in batch and continuous adsorption process. Bioresource Technology 270, 562-569. https://doi.org/10.1016/j.biortech.2018.09.094

Shi P., Chen C., Lu X., Wang P., Mi S., Lu J. and Tong Z. (2023). Preparation, characterization and adsorption potentiality of magnetic activated carbon from *Eucalyptus* sawdust for removal of amoxicillin: Adsorption behavior and mechanism. Industrial Crops and Products 203, 117122. https://doi.org/10.1016/j.indcrop.2023.117122

Sizirici B., Fseha Y.H., Yildiz I., Delclos T. and Khaleel A. (2021). The effect of pyrolysis temperature and feedstock on date palm waste derived biochar to remove single and multi-metals in aqueous solutions. Sustainable Environment Research 31 (9), 1-16. https://doi.org/10.1186/s42834-021-00083-x

Suhaimi N., Koo M.R., Lim C. M., Chou Chao Y.-F., Mahadi A.H., Chiang H.-P., Haji Hassan N.H. and Thotagamuge R. (2022). The use of *Gigantochloa* bamboo-derived biochar for the removal of methylene blue from aqueous solution. Adsorption Science and Technology 2022, 8245797. https://doi.org/10.1155/2022/8245797

Sulaiman N.S., Hashim R., Mohamad Amini M.H., Danish M. and Sulaiman O. (2018). Optimization of activated carbon preparation from cassava stem using response surface methodology on surface area and yield. Journal of Cleaner Production 198, 1422-1430. https://doi.org/10.1016/j.jclepro.2018.07.061

Tee W.T. Li Loh N.Y., Zhang Hiew B.Y., Show P.l., Hanson S., Gan S. and Lee L.Y. (2023). Evaluation of adsorption performance and mechanisms of highly effective 3D boron-doped graphene composite for amitriptyline pharmaceutical removal. Journal of Environmental Management 344, 118363. https://doi.org/10.1016/j.jenvman.2023.118363

Teow Y. and Mohammad A. (2019). A new generation of nanomaterials for water desalination: A review. Desalination 451, 2-17. https://doi.org/10.1016/j.desal.2017.11.041

Thileep Kumar K., Sivagaami Sundari G., Senthil Kumar E., Ashwini A., Ramya M. and Varsha P. (2018). Synthesis of nanoporous carbon with new activating agent for high performance supercapacitor. Materials Letters 218, 181-184. https://doi.org/10.1016/j.matlet.2018.02.017

Üner O. and Bayrak Y. (2018). The effect of carbonization temperature, carbonization time and impregnation ratio on the properties of activated carbon produced from *Arundo donax*. Microporous and Mesoporous Materials 268, 225-234. https://doi.org/10.1016/j.micromeso.2018.04.037

Vargas-Berrones K., Bernal-Jácome L., de León-Martínez L.D. and Flores-Ramírez R. (2020). Emerging pollutants (Eps) in Latin America: A critical review of under studies Eps, case of study -nonylphenol-. Science of Total Environment 726, 138493. https://doi.org/10.1016/j.scitotenv.2020.138493

Wibawa P.J., Nur M., Asy'ari M. and Nur H. (2020). Sem, XRD and FTIR analyses of both ultrasonic and heat generated activated carbon black microstructures. Heliyon 6 (3), E03546. https://doi.org/10.1016/j.heliyon.2020.e03546

Wu J., Yang R., Liu J. and Huang X. (2021). Easy fabrication of aminated graphene oxide functionalized magnetic nanocomposite for efficient preconcentration of phenolic acids prior to HPLC determination: Application in tea-derived wines. Talanta 228, 122246. https://doi.org/10.1016/j.talanta.2021.122246

Wu S., Mao J., Zhang Y., Wang S., Huo M. and Guo H. (2023). Sensitive electrochemical detection of enrofloxacin in eggs based on carboxylated multi-walled carbon nanotubes-reduced graphene oxide nanocomposites: Molecularly imprinted recognition versus direct electrocatalytic oxidation. Food Chemistry 413, 135579. https://doi.org/10.1016/j.foodchem.2023.135579

Yang X.-Q., Yang C.-X. and Yang X.-P. (2013). Zeolite imidazolate framework-8as adsorbent for on-line solid-phase extraction coupled with high-performance liquid chromatography for the determination of tetracyclines in water and milk samples. Journal of Chromatography A 1304, 28-33. http://dx.doi.org/doi:10.1016/j.chroma.2013.06.064

Yorgun S. and Yildiz D. (2015). Preparation and characterization of activated carbons from *Paulownia* wood by chemical activation with H_3PO_4. Journal of the Taiwan Institute of Chemical Engineers 53, 122-131. https://doi.org/10.1016/j.jtice.2015.02.032

Zhang Y., Bian T., Jiang R., Zhang Y., Zheng X. and Li Z. (2021). Bionic chitosan-carbon imprinted aerogel for high selective recovery of Gd (III) from end of life rare earth productions. Journal of Hazardous Materials 407, 124347. https://doi.org/10.1016/j.jhazmat.2020.124347

Zhao W., Chen L. and Jiao Y. (2023). Preparation of activated carbon from sunflower straw through H_3PO_4 activation and its application for acid fuchsin dye adsorption. Water Science and Engineering 16 (2), 192-202. https://doi.org/10.1016/j.wse.2023.02.002

Zhou L., Xu J., Liang X. and Liu Z. (2010). Adsorption of platinum (IV) and palladium (II) from aqueous solution by magnetic cross-linking chitosan nanoparticles modified with ethylenediamine. Journal of Hazardous Materials 182 (1-3), 518-524. https://doi.org/10.1016/j.jhazmat.2010.06.062